Structure, Vol. 9, 627–636, July, 2001, ©2001 Elsevier Science Ltd. All rights reserved. PII S0969-2126(01)00624-4

The Factor VII Zymogen Structure Reveals Reregistration of β Strands during Activation

Charles Eigenbrot,[1,3] Daniel Kirchhofer,[2] Mark S. Dennis,[1] Lydia Santell,[1] Robert A. Lazarus,[1] Jennifer Stamos,[1] and Mark H. Ultsch[1]
[1] Department of Protein Engineering and
[2] Department of Cardiovascular Research
Genentech, Inc.
South San Francisco
California

Summary

Background: Coagulation factor VIIa (FVIIa) contains a Trypsin-like serine protease domain and initiates the cascade of proteolytic events leading to Thrombin activation and blood clot formation. Vascular injury allows formation of the complex between circulating FVIIa and its cell surface bound obligate cofactor, Tissue Factor (TF). Circulating FVIIa is nominally activated but retains zymogen-like character and requires TF in order to complete the zymogen-to-enzyme transition. The manner in which TF exerts this effect is unclear. The structure of TF/FVIIa is known. Knowledge of the zymogen structure is helpful for understanding the activation transition in this system.

Results: The 2 Å resolution crystal structure of a zymogen form of FVII comprising the EGF2 and protease domains is revealed in a complex with the exosite binding inhibitory peptide A-183 and a vacant active site. The activation domain, which includes the N terminus, differs in ways beyond those that are expected for zymogens in the Trypsin family. There are large differences in the TF binding region. An unprecedented 3 residue shift in registration between β strands B2 and A2 in the C-terminal β barrel and hydrogen bonds involving Glu154 provide new insight into conformational changes accompanying zymogen activation, TF binding, and enzymatic competence.

Conclusions: TF-mediated allosteric control of the activity of FVIIa can be rationalized. The reregistering β strand connects the TF binding region and the N-terminal region. The zymogen registration allows H bonds that prevent the N terminus from attaining a key salt bridge with the active site. TF binding may influence an equilibrium by selecting the enzymatically competent registration.

Introduction

Coagulation factor VII (FVII) initiates a cascade that stems blood loss through the generation of a Fibrin clot. Each step in the cascade involves the conversion of a serine protease zymogen into its active form until Prothrombin is converted into Thrombin. Thrombin cleaves Fibrinogen to Fibrin, activates platelets, and also initiates an anticoagulatory process when it combines with Thrombomodulin and activates Protein C. Activated Protein C degrades key cascade components and terminates Fibrin deposition [1]. Full enzymatic activity of FVIIa arises in a complex with the cell bound cofactor, Tissue Factor (TF). The TF/FVIIa complex activates the biologically important substrates factor X (FX), factor IX (FIX), and FVII. Binding of the zymogen FVII to TF increases the rate of its conversion to FVIIa [2]. While many enzymes are capable of converting FVII to FVIIa, FXa is probably the most important one in vivo [3]. In addition to a protease domain with Trypsin homology at its C terminus ("heavy chain"), FVII also has three N-terminal domains, collectively called the "light chain." The first of these is rich in γ-carboxyglutamic acid residues (Gla) and promotes association with cellular membranes. The Gla domain is followed by two epidermal growth factor-like (EGF) domains, the second of which is closely associated with the protease domain. In TF/FVIIa, the Gla and EGF1 domains have the most energetically important TF interactions, although the EGF2 and the protease domains also contact TF [4, 5]. The conversion from FVII to FVIIa involves a proteolytic cleavage between the EGF2 and protease domains.

There is considerable interest in the exact nature of changes in FVII during its conversion from the zymogen to a fully active enzyme in the TF/FVIIa complex. The activation of gastric serine proteases Trypsin and Chymotrypsin is structurally well characterized [6]. Cleavage of a single peptide bond releases a pro-peptide, generates the mature N-terminal residue (Ile16 in FVIIa, according to the Chymotrypsinogen numbering convention), and promotes conformational changes that create the active enzyme. This general scheme has also been seen in crystal structures of Prethrombin2 [7, 8], Plasminogen [9–12], and Complement Factor D [13]. The structural changes arise in a contiguous collection of four peptide segments collectively termed the activation domain [14]. Principal among these peptide segments is the new N terminus itself, which becomes buried with its nonpolar side chain in a hydrophobic environment and its charged α-amino nitrogen atom compensated by a salt bridge to a key aspartic acid side chain from the catalytic active site. Three associated loop segments undergo changes that create the substrate binding cleft. For the structurally characterized zymogen/enzyme pairs, and for a large number of other homologous proteins, this activation scenario provides full enzymatic competence. For FVIIa, however, the "activated" form exhibits poor amidolytic activity (small substrate mimics), is essentially devoid of proteolytic activity (protein substrates), and attains full activity only when associated with TF. The low activity of FVIIa has been ascribed to an incomplete conversion of its activation domain from the zymogen form to the enzyme form [5, 15, 16]

[3] Correspondence: eigenbrot.c@gene.com

Key words: activation; allostery; factor VII; tissue factor; x-ray crystallography; zymogen

Table 1. Structure Statistics for A-183/rF7

Data Collection and Reduction

Resolution (Å)	N_{meas}[1]	N_{ref}[2]	Complete[3]	I/σ	R_{merge}[4]	R_{work}[5]	R_{free}[6]
35.0–4.31	13,883	3,554	99.5	22	0.033	0.204	0.243
4.31–3.42	14,075	3,423	100	23	0.045	0.175	0.179
3.42–2.99	14,044	3,390	99.9	22	0.047	0.186	0.213
2.99–2.71	13,853	3,336	100	18	0.067	0.193	0.226
2.71–2.52	13,788	3,350	99.9	14	0.102	0.212	0.244
2.52–2.37	13,692	3,326	100	10	0.134	0.211	0.228
2.37–2.25	13,553	3,319	100	8.5	0.246	0.229	0.251
2.25–2.15	13,415	3,324	99.8	6.4	0.255	0.241	0.235
2.15–2.07	13,172	3,284	100	5.0	0.364	0.265	0.316
2.07–2.00	12,516	3,318	99.7	3.4	0.422	0.318	0.341
35.0–2.00	135,991	33,624	99.9	9.7	0.062	0.204	0.227

Refinement Statistics

Contents of Model					rms Deviations			
Residues	Atoms[7]	Waters	Ca^{+2}	SO_4^{-2}	Bonds	Angles	B factors (Main)	(Side)
313	2,678 (41)	199	0	1	0.007 Å	1.5°	3.0 Å^2	4.5 Å^2

[1] N_{meas} is the total number of observations measured.
[2] N_{ref} is the number of unique reflections measured at least once.
[3] Complete is the percentage of possible reflections actually measured at least once. The number in parentheses is for the outermost tenth of the data.
[4] $R_{merge} = \Sigma||I| - |\langle I\rangle||/\Sigma|\langle I\rangle|$, where I is the intensity of a single observation and $\langle I\rangle$ the average intensity for symmetry equivalent observations.
[5] $R_{work} = \Sigma|F_o - F_c|/\Sigma|F_o|$, where F_o and F_c are observed and calculated structure factor amplitudes, respectively.
[6] $R_{free} = R_{work}$ for 698 reflections sequestered from refinement.
[7] Number in parentheses is the number of atoms assigned zero occupancy.

because, for instance, the protease domain's N-terminal α-amino nitrogen is more susceptible to chemical modification in the absence of TF than in its presence [17].

Crystallographic analyses of the various "forms" of FVII are confounded by the interplay among allosteric influences exerted at three sites on the protease domain [18]. The first of these sites is the TF binding region, the second is the active site binding cleft, and the third is a region including the protease domain N terminus, which contacts macromolecular substrates. The crystal structure of TF/FVIIa with a covalent inhibitor in the active site revealed details of the interface between TF and FVIIa, including TF contacts on the catalytic domain [4]. It also showed that the TF contact on FVIIa does not include the protease domain's N terminus, so that the influence of TF on the chemical modification of the N terminus must arise from an allosteric effect. Additional allosteric crosstalk is observed between the active site substrate binding cleft and the TF contact region [15, 19, 20] and between the binding cleft and the protease domain N terminus [15]. Recent X-ray structures of FVIIa lacking the TF component [21–23] have shown protease domains similar to those found with TF [4, 24], with a buried N terminus and an almost unchanged TF contact region. However, because these structures also have a substrate mimic in their active site binding clefts, the allosteric connections to the TF contact site and the N terminus may condition them to look like the TF/FVIIa form.

The notion of incomplete zymogen conversion directs attention to the zymogen itself. Our structural interest in this area led us to produce a simplified version of FVII that retains only the EGF2 and catalytic domains (called rF7). We were able to crystallize rF7 in the presence of a peptide, called A-183, which was recently discovered by the use of phage display and selection for binding to TF/FVIIa. Peptide A-183 is a potent inhibitor of TF/FVIIa that binds to a new exosite on the protease domain [25, 26], which is distinct from that of another recently described class of peptide exosite inhibitors [21]. During refinement of the A-183/rF7 complex, we ascertained that the crystals contained the zymogen form of rF7. Because Trypsin-like proteins comprise two β barrel subdomains, we judged the analyses of the A-183 exosite, located in the first β barrel, and the activation domain, located in the second β barrel, to be both distinct and separable. Therefore, we have segregated our reporting of these two aspects, both derived from a single X-ray structure, accordingly. In a separate report, we present the molecular details of the interaction between A-183 and its exosite on rF7 [26]. In this report, we describe the zymogen form of rF7 and characterize an expanded activation domain including an unprecedented new registration between two β strands. Differences in the TF interaction region are large and suggest how TF binding may induce allosteric effects, including the reorganization of the macromolecular substrate exosite and the insertion of Ile16 into its hydrophobic pocket with concomitant formation of the critical salt bridge with Asp194.

Results and Discussion

We began study of these crystals expecting them to contain peptide A-183 and the activated form of the shortened FVII construct rF7 (EGF2 plus protease domains). The molecular replacement search model com-

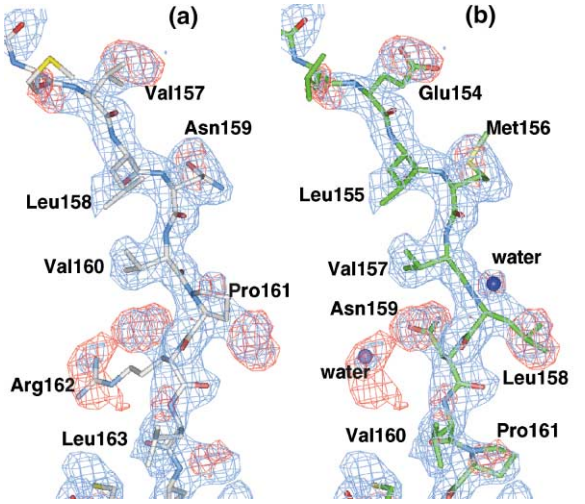

Figure 1. Electron Density Indicates Differences with Prior FVIIa Structures

Electron density maps ($2F_o$-F_c, 1.0 rmsd, blue; F_o-F_c, +3.0 rmsd, red) indicating the 3 residue shift of β strand B2.

(a) Incorrect registration.

(b) Corrected registration from the final model. Maps were calculated with phases from the incorrect registration (R_{work} = 26.2%, R_{free} = 28.2%), with the Arg162 side chain assigned zero occupancy.

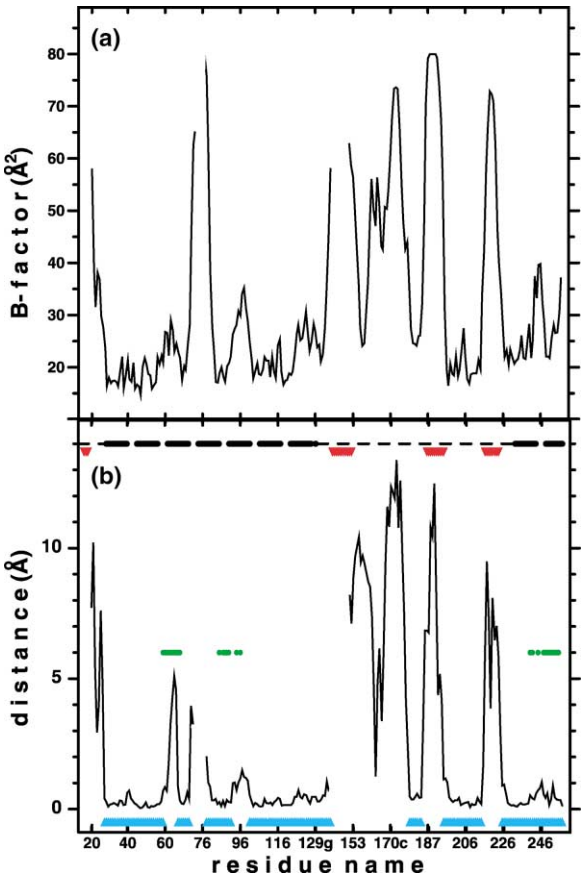

Figure 2. Metrical Comparison with FVIIa

(a) Refined thermal factors (B values) for Cα atoms from the protease domain of A-183/rF7 as a function of those of the primary sequence.

(b) Distance between corresponding Cα atoms after superpositioning of A-183/rF7 and TF/FVIIa [4] as a function of primary sequence. Residues used for superpositioning (upward-pointing triangle, cyan), prototype activation domain residues from Trypsin [14] (downward-pointing triangle, red), residues contacted by peptide A-183 (circle, green), residues in the first β barrel domain (– – –), residues in the second β barrel domain (- - -). Residues 73–75 and 142–150 are disordered and not included in the model. In the first β barrel, there are some differences associated with the presence of peptide A-183, but overall the first β barrels are far more similar than the second β barrels. Superposition of all corresponding Cα atoms yields an rms deviation of 1.1 Å for the first β barrel and 5.2 Å for the second β barrel. Contacts between crystallographic symmetry-related molecules may influence the position of residues 184–193.

posed of these parts from the TF/FVIIa structure permitted a straightforward solution. However, early in the refinement, certain features in the electron density maps led us to suspect that the crystals contained the zymogen instead of the enzyme. Confirmation of the zymogen was made by the single N-terminal amino acid sequence of the single protein band developed in a reducing SDS-PAGE gel run with harvested crystals. If the activating cleavage between the EGF2 and protease domains had occurred, then two SDS bands and two N-terminal sequences would have been found. After the presence of the zymogen became unambiguous, we rebuilt a significant fraction of the model. In this fraction, correspondence between model and electron density was poor (Figure 1, Table 1). The very significant differences between the rF7 protease domain and prior FVIIa structures are evident in Figure 2a, which recapitulates the analysis of Trypsin/Trypsinogen by Huber and Bode [14] and their characterization of the prototypical activation domain. The significant differences between A-183/rF7 and prior TF/FVIIa and FVIIa structures are mostly found within the second β barrel, which contains the activation domain (Figure 3). Differences within the first β barrel are clearly associated with the presence of A-183 [26]. Given these considerations, we argue that the structure of each β barrel is largely independent of the other and that their analyses are separable. Here we concentrate on the second β barrel.

The Canonical Activation Domain

Striking differences in the second β barrel are found in comparison to prior FVIIa structures ([4, 21–24]; Figures 2a and 3). Despite the presence of 5 mM Ca^{+2} in the crystallization medium, the high-affinity calcium site in the Glu70-Glu80 loop is not occupied, and part of the loop is disordered. Residues 142–150 are also too poorly ordered to be traced. The poor ordering in the calcium binding loop may derive from the disruption of H bonds with neighboring residues, which are present in TF/FVIIa. The disruption is caused by changes in the Cys22-Cys27 loop (see below). The Cα atoms of activation domain loops 184–193 and 215–224 shift by up to 12 Å (Figure 2a). These two loops have high thermal factors (Figure 2b) and were fit into feeble electron density. Despite the presence of 5 mM benzamidine in the crystallization medium, the S1 substrate pocket is not occupied. Indeed, the S1 pocket does not exist due to shifts in

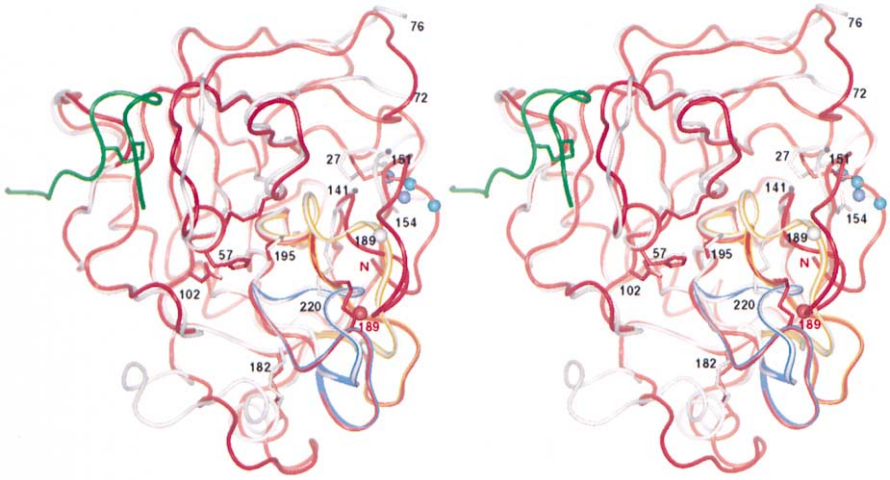

Figure 3. Superposed zymogen and Enzyme

Stereoview of protease domains from A-183/rF7 (white) and TF/FVIIa (red). A-183 is in green. Some changes associated with binding of A-183 are apparent, but the first β barrels (upper left) are largely the same. The most significant differences are in the second β barrel in the lower right. The catalytic triad (Asp102, His57, and Ser195) and selected residues are labeled in black. When labeled residues from the two protease domains are widely separated, red labels are used for TF/FVIIa. Activation domain loops are highlighted in blue (184a–197) or yellow (214–225). Another activation domain loop (142–152) is disordered in A-183/rF7 but is present for TF/FVIIa. Spheres represent the Cα atom of Asp189 from each structure. The side chain of Glu154 from A-183/rF7 shows H bonding to main-chain nitrogen atoms (dark blue spheres) of residues 21 and 22. The corresponding nitrogen atoms of TF/FVIIa are in light blue.

relevant sections of the protein. For example, Asp189, which is at the bottom of the S1 pocket in TF/FVIIa, is shifted by 12 Å in rF7.

The most conspicuous differences, however, occur in the N-terminal residues 16–27 and the β strand B2 (residues 153–162 [12]). Residues 16–19 are too poorly ordered to be traced, as are residues at the end of the EGF2 domain to which they are still connected in the zymogen. The poor ordering of residues 16–19 is significant because of the key structural role played by a salt bridge between the α-amino nitrogen of Ile16 and the side chain of Asp194. This salt bridge is critical in the formation of a competent catalytic site in the active enzyme. We are able to fit residues starting at Lys20, but the main-chain trace of the loop between Cys22 and Cys27 is approximately reversed relative to TF/FVIIa (Figure 4). As a result, Lys20 is farther away from Asp194 and closer to Lys143L, to which it is connected via 13 intervening amino acids. Not unexpectedly, these 13 residues are completely disordered in the present crystal. Of these 13 residues, the 9 that are formally part of the light chain after activation are also disordered in all prior structures of FVIIa. Additionally, an inherent flexibility and solvent exposure for this segment in FVII is consistent with the requirement that it be available to another enzyme's active site for the activating cleavage reaction to occur.

Reregistered β Strand

A quite unanticipated feature in this structure is the β strand B2 (residues 153–162). This strand lies between the unresolved loop 142–150 and a short α helix (α1) that contains part of the TF binding region [5]. It shares main-chain-to-main-chain H bonds with β strand A2 (residues 134–140). In TF/FVIIa, β strand B2 also has main-chain H bonds with residues 20 and 22. In the present structure, residues 151–168 are shifted by 3 amino acid residues toward the C terminus relative to TF/FVIIa (Figure 5). Thus, the loop preceding β strand B2, despite not being resolved, must be 3 amino acids shorter than in prior structures. The three residues added at the C-terminal end of this strand are largely taken up before Cys168 by addition to the N-terminal end of the α helix α1. The position of β strand A2 does not differ, and the pattern of inter-β strand main-chain

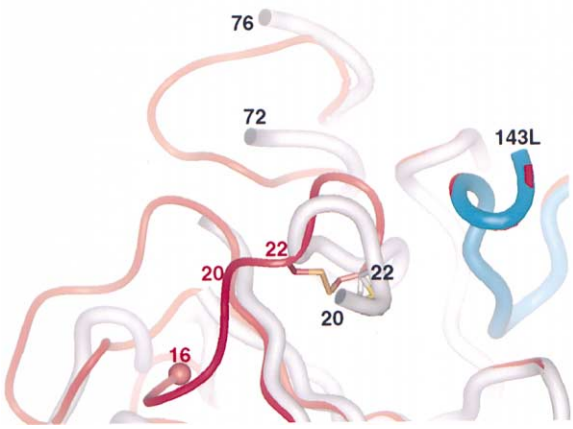

Figure 4. Differences in the N-Terminal Region

A-183/rF7 is in white (protease domain) and blue (EGF2), TF/FVIIa is in red. The 13 amino acid connection between residues Lys20 and Lys143L in A-183/rF7 is intact, based on N-terminal sequencing of the single SDS/PAGE band, but it is too poorly ordered to be traced. The backbone traces of residues 22–27 are in opposite directions. The poor ordering of residues 72–76 in A-183/rF7 is associated with the new placement of the Glu26 side chain.

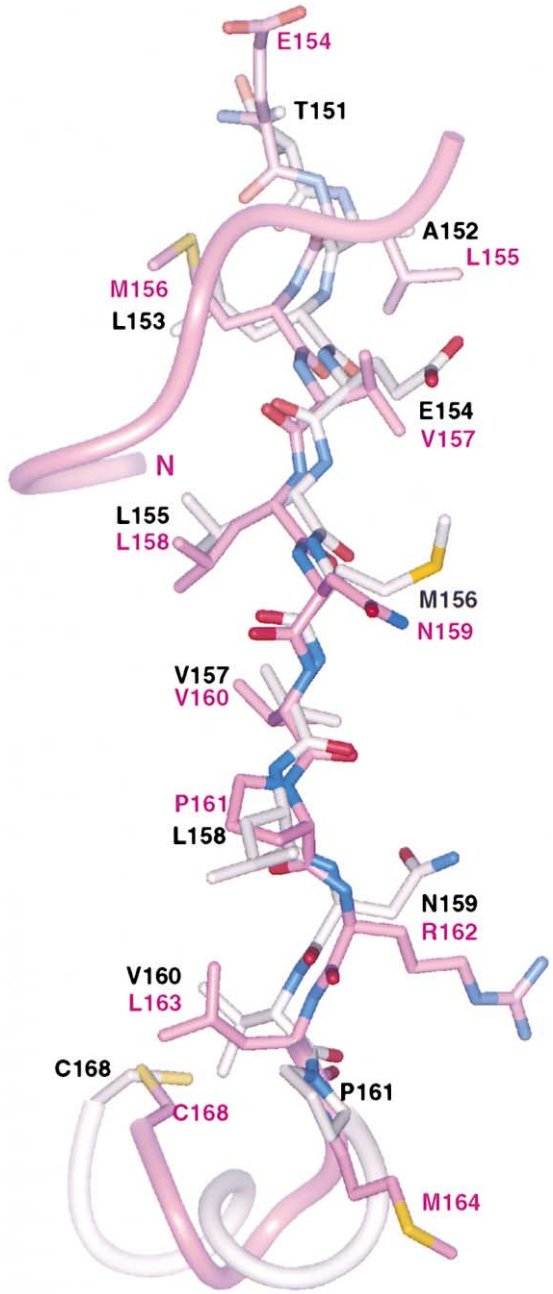

Figure 5. The Shifting β Strand

Comparison of β strand B2 in A-183/rF7 and TF/FVIIa. Worm and carbon atoms of A-183/rF7 are white. Worm and carbon atoms of TF/FVIIa are pink. The pink worm draped across the top of B2 represents residues 16–23 of TF/FVIIa (these residues are either disordered or in different positions in A-183/rF7). The close correspondence of main-chain atoms allows H bonds with the companion β strand A2 in both structures. The two different registrations of B2 share a similar pattern of polar and nonpolar side chains (except Glu154/Val157), but solvent accessibility calculations show a more favorable segregation into suitable environments in TF/FVIIa (pink). Changes in the helical region preceding Cys168 disrupt the TF binding region of the protease domain in A-183/rF7.

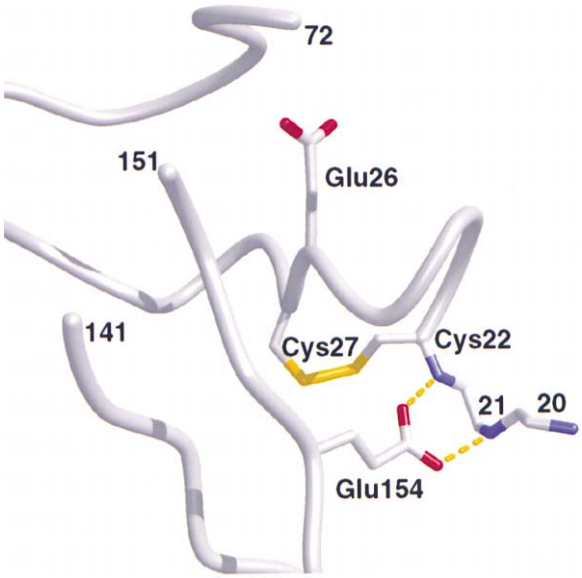

Figure 6. H Bonds between Glu154 and Residues 21 and 22 in A-183/rF7

With these H bonds, a newly created N-terminal Ile16 could not reach into the insertion site and form a salt bridge with Asp194. Changes in the Cys22-Cys27 loop cause Glu26 to displace residues 71 and 72 relative to TF/FVIIa, and prevent main-chain H bonds between residues 71 and 73 and residues at the top of β strand B2. This may explain residues 73–75 being unresolved.

H bonds does not differ from earlier FVIIa structures, but the residues complementing the β strand A2 are all shifted by 3 residues. In addition to the eight main-chain-to-main-chain H bonds, the rF7 β strand B2 has H bonds from the side chain of Glu154 to the amide nitrogen atoms of residues 21 and 22 (Figure 6) and between the side chain of Asn159 and the side chains of Ser136 and His199. In TF/FVIIa, all of the H bonds beyond the eight main-chain-to-main-chain ones are different. With the additional H bonds involving N-terminal residues Ile16 and Val17, there are a greater number in TF/FVIIa than in rF7 (15 versus 12).

The two structures also differ in the degree of solvent exposure of nonpolar side chains from this region. Leu155 displays 36% solvent accessibility in rF7 (relative to an extended Gly-Leu-Gly tripeptide), but it displays only 2% in TF/FVIIa. Leu158 undergoes a change from 40% in rF7 to 4% accessibility in TF/FVIIa. Similar differences apply to residues Pro161 and Leu163. Met156 is 51% solvent accessible in rF7 and 13% in FVIIa. On the other hand, polar side chains tend to be more solvent accessible after registration to the TF/FVIIa form. Asn159 has a low solvent accessibility in rF7 (16%) relative to TF/FVIIa (38%) due to side-chain H bonds in rF7 that are absent in TF/FVIIa (see above). For the same reason, Glu154 has a lower accessibility in rF7 (19%) than in FVIIa (36%). Except for the H bonds lost by Glu154 and Asn159, the free energy associated with these differences favors TF/FVIIa.

TF Binding Region

Very significant differences exist for residues 160–176 (Figure 2a), including residues Met164, Asp167, and Gln166, which are part of the TF binding region on the protease domain ([4]; Figure 7). The differences at the

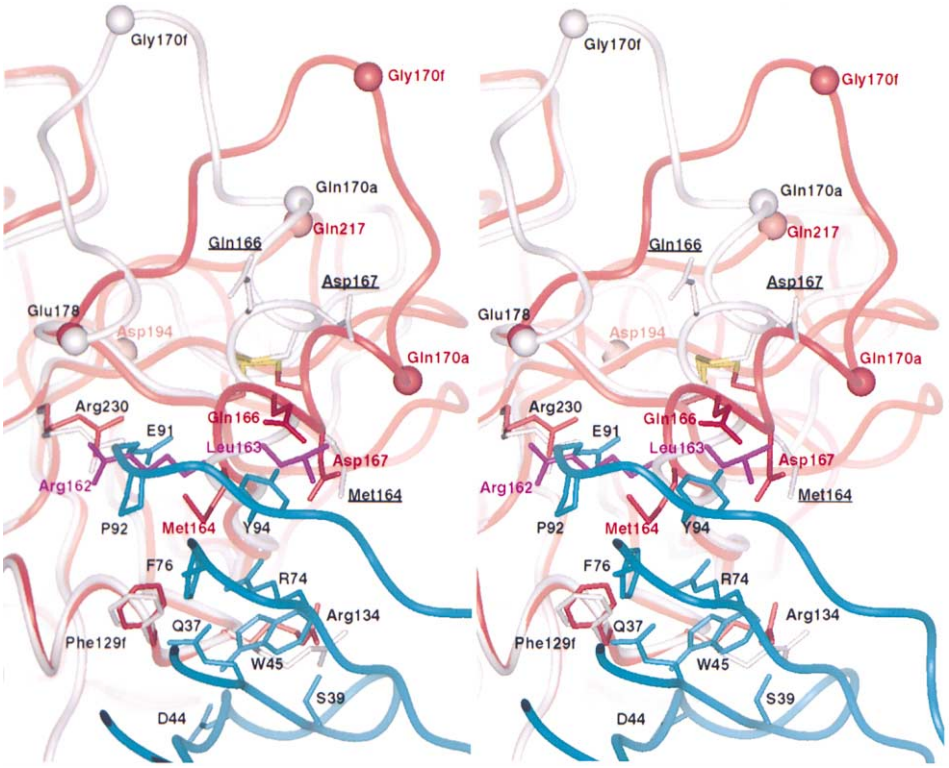

Figure 7. Stereoview of Tissue Factor Binding Region in A-183/rF7 and TF/FVIIa

TF is in blue with single-letter amino acid codes. A-183/rF7 is in white, and FVIIa is in red, both with three-letter amino acid codes. Underlined are rF7 residues that are important contacts for TF in TF/FVIIa but differ significantly in the two structures. Purple side chains are from rF7 and would cause steric clashes with TF if unchanged. For reference, Asp194 Cα is labeled. Cystine Cys168–Cys182 is included from both structures, and the comparison shows the opposite handedness.

start of this segment are associated with the extra three amino acids from the preceding β strand, B2. At residue Cys168, the correspondence with TF/FVIIa is sufficiently restored (the distance between corresponding Cys168 Cα atoms is 3.4 Å) so that the disulfide bond still forms with the almost unchanged Cys182. The differences in the TF binding region not only withdraw residues that are part of the TF interaction surface in TF/FVIIa but also would prevent TF from assuming its normal position relative to the rest of the protease domain. In particular, residues Arg162 and Leu163 would cause steric clashes with TF residues Glu91/Pro92 and Tyr94, respectively, if TF maintained the same structure displayed in the TF/FVIIa complex ([4]; Figure 7). The structures of TF without FVIIa [27] and in the TF/FVIIa complex are very similar, and this similarity makes large conformational changes in TF due to interaction with FVII unlikely.

The Activation Domain of FVII

In addition to the four elements composing the activation domain in Trypsin and Chymotrypsin, FVII also shows differences in the short α helix α1 (containing part of the TF binding region), the region centered on 170f (called the methionine loop), the β strand B2, the Cys22-Cys27 loop, and the 70–78 loop. These additional elements are associated with specific features of the FVII amino acid sequence and are coupled to each other and the four canonical elements either through the covalent backbone or by proximity. The methionine loop primary sequence in FVII is longer than other structurally characterized zymogen/enzyme pairs, and this allows greater conformational variability. Interestingly, recent results demonstrate that the length of the FVII methionine loop has functional relevance [28].

We have characterized the FVII zymogen structure by using a shortened construct that lacks the Gla and EGF1 domains. Similar to how it is found in TF/FVIIa [29], intact FVIIa is elongated in solution. This fact, in combination with the small or zero difference between the affinities of FVII and FVIIa for TF [17, 30–32], suggests that zymogen FVII is elongated even in the absence of TF. However, there is evidence of activation-dependent change in the EGF1 domain [33], and this raises the possibility that the missing domains influence the protease domain in FVII. Definitive judgement on the validity of the truncated structure must await structural information on full-length FVII.

Important Role of Glu154 in the zymogen

The H bonds involving the Glu154 side chain may be especially important in the activation process. With this H bonding arrangement (Figure 6), a newly formed N-terminal α-amino nitrogen atom cannot reach Asp194 and establish the key salt bridge because residues 21 and 22 are held too far away (Figure 3). In the TF/FVIIa registration of B2, this restraint does not exist because

Glu154 is in the 142–154 loop and Val157 occupies its former position. The glutamate in FVII is unusual for position 154 among mammalian Trypsin-like serine protease sequences, although there is not strong conservation of any amino acid. The available murine, canine, bovine, rhesus monkey, and rabbit FVII sequences are equivocal on the question of importance for this glutamate. The bovine FVII sequence has lysine, canine has glutamine, and the others are glutamate. The possibility that bovine zymogen FVII is fundamentally more enzyme-like by virtue of the Lys at 154 would help explain the esterase activity ascribed to it [34]. Some related proteins of known structure have glutamate at position 157, which is the position structurally analogous to Glu154 in the rF7 zymogen [10, 12, 35, 36]. None of these glutamate residues has H bonds like those in rF7.

A residue-specific, allosteric role for Glu154 has been described [37]. The Glu154 side-chain is required for the transmission of an allosteric influence from the macromolecular substrate exosite to the active site cleft. The monoclonal antibody F3-3.2A recognizes an epitope on the protease domain that includes the N-terminal region, parts of the Ca^{+2} binding loop (residues 70–80), and Met156 on β strand B2 [38]. Residue Glu154 is not part of its epitope in FVIIa [37], but its importance in FVII has not been reported. Interestingly, the antibody binds more tightly to FVIIa without TF than to TF/FVIIa [38] (approximately 3-fold more tightly). This difference apparently arises from the zymogen-like features present in the FVII/FVIIa mixture against which it was raised because it displays 2-fold tighter binding to FVII than to FVIIa [38]. The antibody also reduces the amidolytic activity of TF/FVIIa through an allosteric effect, probably the induction of, or preference for, zymogen-like features. The allosteric reduction of amidolytic activity is almost eliminated when Glu154 is mutated to alanine [37], and this finding is consistent with the Glu154 side chain being important for zymogen-like features recognized by F3-3.2A.

TF and "zymogenicity" in FVIIa

The formally activated FVIIa has a significant dependence on TF for catalytic competence. For macromolecular substrates, membrane bound or synthetic vesicle bound TF enhances FVIIa function by about 10^5-fold [39, 40]. Most of this dependence is explained by the membrane localization of TF/FVIIa and the macromolecular substrate [41] and by substrate interactions directly with TF [42]. However, there has been no explanation for the purely allosteric increase (approximately 50-fold) remaining for small peptidyl substrates [19, 20]. A crystal structure of FVIIa alone would help address this question but is so far not available, partly because substrate-like inhibitors are used for limiting unwanted autolysis during purification and crystallization. The presence in known FVIIa structures of either a substrate mimic [21–23] or both a substrate mimic and TF [4, 24] has precluded analysis of FVIIa with no allosteric influences. The distinguishing feature of the pertinent molecular species is an N terminus that is accessible to carbamylation [17] and that therefore seems not to have established the key Asp194 salt bridge, which conditions the active site for catalysis.

A functional kinship between zymogen FVII and FVIIa without TF has been recognized because the first is inactive and the second is poorly active in comparison to TF/FVIIa. To the extent that there is also a *structural* kinship, the zymogen structure allows us to speculate on how TF turns FVIIa into a true enzyme. Of the structural rearrangements for conversion to fully active TF/FVIIa that are indicated by the zymogen structure, the two that are unique to the FVII system are the remodeling of the TF binding region and the reregistration of β strand B2. Perhaps one or both of these is the origin of TF's allosteric influence on the active site and N terminus.

In attempting to characterize FVIIa without TF by interpolation between the zymogen and TF/FVIIa, the energetic requirement of the transition is an important guidepost. The energetic requirement of rF7 activation is not known, nor is it known for authentic full-length FVII. However, a useful surrogate measurement is available. Despite conflicting data on the difference in affinity of TF for the zymogen and the enzyme (0- to 10-fold effect on K_D; [17, 30–32]), in no case is a large difference indicated. Therefore, adoption of the TF/FVIIa-like TF binding region by the zymogen requires only about 1 kcal/mol or less. Because FVIIa without TF possesses low but non-zero amidolytic activity, the activation barrier to formation of the competent active site must not be prohibitive. These data have been used to argue that an equilibrium exists between relatively zymogen-like and relatively TF/FVIIa-like forms of FVIIa [15, 16] but equally allow a similar equilibrium for the zymogen.

In contrast, reregistration of β strand B2 would seem to require a considerable activation energy. The details of the molecular process of transition from one registration to the other is open to speculation. To our knowledge, it is unprecedented. However, the FVII sequence is particularly amenable to the 3 residue registration shift in that it contains a Leu-X-Val-Leu-X-Val tripeptide repeat. The reregistration to a TF/FVIIa-like B2 permits additional H bonds to form and results in a more favorable segregation of nonpolar and polar side chains (see above). A roughly analogous conformational change occurs during inhibition of proteases by serpins, including the insertion of a newly formed β strand into an existing β sheet [43]. There is evidence that such an insertion is reversible under mild conditions [44]. Based on these observations, it is possible that reregistration occurs under mild conditions as part of an equilibrium.

Furthermore, we are attracted to a hypothesis that the rearrangement of the TF binding region and the reregistration of β strand B2 are linked, in the sense that one requires the other. A competent TF binding region seems likely to necessitate expulsion of the three "extra" residues into β strand B2. Such a linkage is supported by the affinity loss between antibody F3-3.2A and FVIIa when TF is present [38] because the antibody epitope includes residues changed by the B2 reregistration. However, F3-3.2A binds with equal affinity to zymogen FVII with and without TF [38]. These results support the hypothetical linkage in FVIIa but argue that it is absent in the zymogen. If the linkage is present in FVIIa, then either the linkage is absent from the zymogen or F3-3.2A accommodates the linkage-induced changes in some energetically neutral manner that is not available with

FVIIa. Given the small size of the difference (approximately 3-fold) in affinity between the antibody and FVIIa caused by TF, an energetically neutral accommodation of the zymogen seems possible. Alternatively, the TF binding region on zymogen FVII could be different from the one on FVIIa, and this or some other difference could in some way preclude the linkage to B2 that seems present in FVIIa. The resolution of this apparent discrepancy will determine in which molecules (FVII and/or FVIIa) and by which means (via linkage to B2 or not) TF binding exerts an allosteric influence on the N-terminal region. According to our linkage hypothesis, the Glu154→Ala FVIIa mutant would have a tighter affinity for TF than would the wild type, and it would have greater amidolytic activity than the wild type. Shobe et al. have shown the first point to be marginally true, but the second point seems not to be the case [37].

Conclusion

The notion that TF selects an "active" form of FVIIa from an equilibrium with an "inactive" form is well established [15, 16]. The zymogen structure adds new features to speculation regarding the molecular details of this scheme. As for related zymogens, FVII alone is not a catalyst because there is a poorly formed or absent substrate binding cleft and no N-terminal α-amino nitrogen to condition the active site via a salt bridge with Asp194. For FVII, the energetically favored form of the zymogen is probably the one characterized in this report. Three caveats to this assertion should be kept in mind. Firstly, our structure was determined in complex with the peptide A-183. However, the binding site for A-183 is far from most elements of FVII's activation domain and is in a different tertiary structural component of the protease domain. Secondly, some structural details of one of the activation domain loops may have been selected by intermolecular contacts within the crystal lattice. Any structural effects of the intermolecular contacts are probably not significant in the following outline. Finally, our structure lacks the Gla and EGF1 domains, which are affected by events in the protease domain [33]. Without a structural explanation for this connection, it is difficult to gauge how, or if, the absent domains would have altered our result.

The key feature of this zymogen structure is a unique registration of β strand B2 that permits Glu154 H bonds with residues near the scissile Arg15-Ile16 peptide bond and, according to the linkage hypothesis, precludes TF binding. Because the energetic cost seems small, we suggest there is also a significant minority of FVII molecules that have a reregistered B2, resulting in loss of the Glu154 H bonds with residues 21 and 22 and a competent TF binding region. If TF binds to FVII, it would select from this population. When the TF/FVII complex undergoes the activating cleavage reaction, the N terminus–Asp194 salt bridge can be formed immediately, and a fully competent enzyme results. Alternatively, when FVII is cleaved before association with TF, the equilibrium mixture would include a population in which H bonds between Glu154 and residues 21 and 22 prevent the formation of the N terminus–Asp194 salt bridge. The catalytic activity of this equilibrium mixture would then be low due to the presence of this incompetent form.

Biological Implications

The importance of the balance between thrombosis and hemostasis is suggested by its highly regulated nature and cofactor dependency. A major regulatory aspect of the initial event in the extrinsic coagulation cascade can now be rationalized. It has long been known that the serine protease coagulation factor VII/VIIa is present in circulating blood but is largely inactive. Even the nominally activated FVIIa retains zymogen character, in contrast to related enzymes, such as Trypsin, in which activating cleavage(s) create a fully active enzyme. Upon exposure to the extravascular environment or to certain membranes within atherosclerotic plaques, factor VIIa forms a complex with the cell-surface bound Tissue Factor, and this combination proceeds to activate downstream clotting factors as well as form more FVIIa. The Tissue Factor part of this complex helps localize and orient FVIIa and also guides substrates to productive interactions with the FVIIa active site. The exact nature of an additional long-range allosteric effect transmitted from the TF binding region to the FVIIa catalytic active site has been subject to conjecture. The structure of zymogen FVII reported here includes an unprecedented refolding relative to the TF bound form of FVIIa. A single strand of secondary structure imbedded in the protein structure must shift by 3 amino acid residues, or about 12 Å, to attain the active enzyme structure. This shift eliminates an impediment to full activity, and a key conformational change accompanying Trypsin family enzyme activation becomes possible. Therefore, we hypothesize that the previously proposed equilibrium between zymogen-like FVIIa and enzyme-like FVIIa is shifted toward the enzyme-like species in TF/FVIIa because a well-formed TF binding region requires the shifted strand, which, in turn, permits formation of the fully competent active site.

Experimental Procedures

Production of rF7 and A-183

A recombinant transfer vector, gp67ssFVII, consisting of the gp67 signal sequence attached to FVII cDNA containing the EGF2 and protease domains only (residues Ile90L to Pro257) was constructed. Similar simplifications of related enzymes are known [45]. The protein of interest, rF7, is expressed as a gp67 signal peptide fusion protein under the control of the strong baculovirus polyhedrin promoter. To generate gp67ssFVII, we used a baculovirus transfer vector, pAcGP67 (PharMingen, San Diego, California), and full-length human FVII cDNA as templates in a polymerase chain reaction (PCR) to generate two products with the appropriate sequence. We performed a second PCR reaction to anneal these two products and to insert a SpeI restriction site at the 5′ end and an EcoRI site at the 3′ end. All PCR amplifications were for 35 cycles, with denaturation for 1 min at 95°C, annealing for 1 min at 55°C, and extension at 72°C for 1 min. The nucleotide sequences generated by PCR were confirmed by DNA sequencing with the dye terminator method (PE Applied Biosystems, Foster City, California). The PCR product was cloned into the SpeI and EcoRI sites of pAcGP67.

Spodoptera frugiperda insect cells, *Sf*9, were plated onto 6-well dishes and transfected at 60%–70% confluence. The cells were exposed to 1.5 μg gp67ssFVII plasmid, 175 ng BaculoGold™ linearized DNA (PharMingen, San Diego, California), and 10 μg Lipofectin reagent (Life Technologies, Rockville Maryland) in serum-free Hink's TNM-FH supplemented GRACE's insect media (JRH Biosciences, Lenexa, Kansas) overnight at room temperature with rotation. After incubation, the transfection medium was replaced with Hink's sup-

plemented with 10% fetal bovine serum (Hyclone, Logan, Utah) for 4–5 days at 28°C for production of the virus. The virus was amplified 2–3 times by the infection of *Sf*9 cells with cell supernatants in monolayer cultures. The amplified viral supernatant was used for the infection of High Five™ cells (Invitrogen, San Diego, California and Expression Systems, Woodland, California), which express protein more efficiently. Briefly, High Five™ cells in suspension cultures were infected with the amplified virus, and expression was allowed to proceed for 3–5 days. For the removal of cell debris, the cell suspension was centrifuged at 1400 × g for 20 min at 4°C. The supernatant was made 10 mM in benzamidine and 0.02% in sodium azide and then loaded onto an affinity column. The affinity column consisted of a Protein Z fusion with an A-series peptide (A-100-Z[25]) coupled to CNBr sepharose, equilibrated, and washed with 0.15 M NaCl, 20 mM sodium Bis-Tris (pH 6.5), and 1 mM benzamidine. Protein was eluted with 3% acetic acid, concentrated, and run through a Superdex 75 column equilibrated in 0.15 M NaCl, 20 mM sodium Bis-Tris (pH 6.5), and 1 mM benzamidine. The final yield was 0.2–0.4 mg/liter. Peptide A-183 was prepared as reported [25].

Crystallization and Structure Determination

Crystals formed overnight in hanging drops containing 100 mM Hepes (pH 7.5), 850 mM ammonium sulfate, 7.5% glycerol, 0.85% PEG 400, 5 mg/mL rF7, 5 mM benzamidine, 5 mM Ca^{+2}, and 0.3 mg/mL A-183. Crystals were collected, rinsed in reservoir, and run on a reducing SDS/PAGE gel, revealing only one band at 42 kDa. This band was subjected to N-terminal sequencing and showed one N terminus, that of the EGF2 domain of FVII (Ile-[no data]-Val-Asn-Glu-Asn-Gly-Gly-Cys-Glu). For data collection, crystals were macroseeded multiple times. A crystal was harvested and flash frozen in liquid nitrogen, and data were collected on an ADSC Quantum4 CCD detector at beamline 5.0.2 at the Advanced Light Source (ALS). Data reduction was performed in space group $P2_12_12_1$ with a = 67.44 Å, b = 84.51 Å, and c = 84.84 Å by the use of DENZO/SCALEPACK [46] and elements of the CCP4 suite [47].

The structure was solved by molecular replacement (AMORE [48]) with the EGF2 and catalytic domains from the TF/FVIIa complex (Protein Data Bank code 1DAN). Of the reflections between 20 and 2 Å resolution, 2% (698) were sequestered from all refinements. The rigid body-refined molecular replacement solution yielded working and free R values of 46.0 and 47.2, respectively, for data 10.0–3.0 Å. A $2F_o$-F_c map indicated changes in 6 residues centered on Trp61 of the protease domain. Extra density suggesting a peptide was discerned in the region identified as the A-exosite [26]. The $2F_o$-F_c density was weak for several parts of the catalytic domain, notably residues 16–26, 73–79, 143–151, 168–170a, 170c–170g, 184–188, and 219–224. Either these residues were removed entirely from the model or their occupancies were set to zero. Through several cycles of refinement (X-PLOR98, MSI, San Diego) and map inspection (Xtal-View [49]), peptide A-183 was easily built into good electron density, the region 60a-63 was easily rebuilt so that it was shifted from the original position, and weak density was used for rebuilding the residues removed at the start, except for residues 16–19, 142–150, and 73–75. The EGF2 domain was discerned from residue Ile90L to Lys143L. Significant and unprecedented changes at the Cys22-Cys27 cystine and in the β strand composed of residues 151–160 were made in response to unambiguous features in F_o-F_c maps (Figure 1). A check of main chain torsion angles [50] found 87% in most-favored and 12% in additionally allowed regions. Residue Ala221a is in a disallowed region ($\phi,\psi = 75°, 167°$). The final R value for all data is 21.2% (Table 1).

Acknowledgments

We are grateful to Thomas Earnest and Keith Henderson of ALS for data collection assistance; to David Banner, Rick Artis, Sarah Hymowitz, Felix Vajdos, Robert Kelley, and Bart de Vos for helpful discussions; to Han Chen for fermentation support; to Jake Tropea for N-terminal sequencing; to Martin Roberge for peptide production; and to Martin Struble for peptide purification. The Advanced Light Source is supported by the Director, Office of Science, Office of Basic Energy Sciences, Materials Sciences Division of the U.S. Department of Energy under contract number DE-AC03-76SF00098 at Lawrence Berkeley National Laboratory.

Received: March 21, 2001
Revised: June 8, 2001
Accepted: June 11, 2001

References

1. Davie, E.W., Fujikawa, K., and Kisiel, W. (1991). The coagulation cascade: Initiation, maintenance, and regulation. Biochemistry *30*, 10363–10370.
2. Nemerson, Y., and Repke, D. (1985). Tissue factor accelerates the activation of coagulation factor VII: the role of a bifunctional coagulation cofactor. Thromb. Res. *40*, 351–358.
3. Butenas, S., and Mann, K.G. (1996). Kinetics of human factor VII activation. Biochemistry *35*, 1904–1910.
4. Banner, D.W., et al., and Kirchhofer, D. (1996). The crystal structure of the complex of blood coagulation factor VIIa with soluble tissue factor. Nature *380*, 41–46.
5. Kirchhofer, D., and Banner, D.W. (1997). Molecular and structural advances in tissue factor-dependent coagulation. Trends Cardiovas. Med. *7*, 316–324.
6. Creighton, T.E. (1984). *Proteins. Structure and Molecular Properties*. (New York: W.H. Freeman and Company).
7. Vijayalakshmi, J., Pagmanabhan, K.P., Mann, K.G., and Tulinsky, A. (1994). The isomorphous structures of prethrombin2, hirugen-, and PPACK-thrombin: changes accompanying activation and exosite binding to thrombin. Protein Sci. *3*, 2254–2271.
8. Malkowski, M.G., Martin, P.D., Guzik, J.C., and Edwards, B.F.P. (1997). The co-crystal structure of unliganded bovine α-thrombin and Prethrombin-2: movement of the Tyr-Pro-Pro-Trp segment and active site residues upon ligand binding. Protein Sci. *6*, 1438–1448.
9. Wang, X., Lin, X., Loy, J.A., Tang, J., and Zhang, X.C. (1998). Crystal structure of the catalytic domain of human plasmin complexed with streptokinase. Science *281*, 1662–1665.
10. Parry, M.A., et al., and Bode, W. (1998). The ternary microplasmin-staphylokinase-microplasmin complex is a proteinase-cofactor-substrate complex in action. Nat. Struct. Biol. *5*, 917–923.
11. Peisach, E., Wang, J., de los Santos, T., Reich, E., and Ringe, D. (1999). Crystal structure of the proenzyme domain of Plasminogen. Biochemistry *38*, 11180–11188.
12. Wang, X., Terzyan, S., Tang, J., Loy, J.A., Lin, X., and Zhang, X.C. (2000). Human plasminogen catalytic domain undergoes an unusual conformational change upon activation. J. Mol. Biol. *295*, 903–914.
13. Jing, H., Macon, K.J., Moore, D., DeLucas, L.J., Volanakis, J.E., and Narayana, S.V. (1999). Structural basis of profactor D activation: from a highly flexible zymogen to a novel self-inhibited serine protease, complement factor D. EMBO J. *18*, 804–814.
14. Huber, R., and Bode, W. (1978). Structural basis of the activation and action of trypsin. Acc. Chem. Res. *11*, 114–122.
15. Higashi, S., Matsumoto, N., and Iwanaga, S. (1996). Molecular mechanism of tissue factor-mediated acceleration of factor VIIa activity. J. Biol. Chem. *271*, 26569–26574.
16. Dickinson, C.D., Kelly, C.R., and Ruf, W. (1996). Identification of surface residues mediating tissue factor binding and catalytic function of the serine protease factor VIIa. Proc. Natl. Acad. Sci. USA *93*, 14379–14384.
17. Higashi, S., Nishimura, H., Aita, K., and Iwanaga, S. (1994). Identification of regions of bovine factor VIIa essential for binding to tissue factor. J. Biol. Chem. *269*, 18891–18898.
18. Ruf, W., and Dickinson, C.D. (1998). Allosteric regulation of the cofactor-dependent serine protease coagulation factor VIIa. Trends Cardiovasc. Med. *8*, 350–356.
19. Butenas, S., Ribarik, N., and Mann, K.G. (1993). Synthetic substrates for human factor VIIa and factor VIIa–tissue factor. Biochemistry *32*, 6531–6538.
20. Neuenschwander, P.F., Branam, D., and Morrissey, J.H. (1993). Importance of substrate composition, pH and other variables on tissue factor enhancement of factor VIIa activity. Thromb. Haemost. *70*, 970–977.

21. Dennis, M.S., et al., and Lazarus, R.A. (2000). Peptide exosite inhibitors of factor VIIa as anticoagulants. Nature *404*, 465–470.
22. Kemball-Cook, G., Johnson, D.J.D., Tuddenham, E.G.D., and Harlos, K. (1999). Crystal structure of active site-inhibited human coagulation factor VIIa (des-Gla). J. Struct. Biol. *127*, 213–223.
23. Pike, A.C.W., Brzozowski, A.M., Roberts, S.M., Olsen, O.H., and Persson, E. (1999). Structure of human factor VIIa and its implications for the triggering of blood coagulation. Proc. Natl. Acad. Sci. *96*, 8925–8930.
24. Zhang, E., St. Charles, R., and Tulinsky, A. (1999). Structure of extracellular tissue factor complexed with Factor VIIa inhibited with a BPTI mutant. J. Mol. Biol. *285*, 2089–2104.
25. Dennis, M.S., Roberge, M., Quan, C., and Lazarus, R.A. (2001). Selection and characterization of a new class of peptide exosite inhibitors of coagulation factor VIIa. Biochemistry, in press.
26. Roberge, M., Santell, L., Dennis, M.S., Eigenbrot, C., Dwyer, M.A., and Lazarus, R.A. (2001). A novel exosite on coagulation factor VIIa and its molecular interactions with a new class of peptide inhibitors. Biochemistry, in press.
27. Muller, Y.A., Ultsch, M.H., and de Vos, A.M. (1996). The crystal structure of the extracellular domain of human tissue factor refined to 1.7 Å resolution. J. Mol. Biol. *256*, 144–159.
28. Soejima, K., Mizuguchi, J., Yuguchi, M., Nakagaki, T., Higashi, S., and Iwanaga, S. (2001). Factor VIIa modified in the 170 loop shows enhanced catalytic activity but does not change the zymogen-like property. J. Biol. Chem. *276*, 17229–17235.
29. Ashton, A.W., Boehm, M.K., Johnson, D.J., Kemball-Cook, G., and Perkins, S.J. (1998). The solution structure of human coagulation factor VIIa in its complex with tissue factor is similar to free factor VIIa: a study of a heterodimeric receptor-ligand complex by X-ray and neutron scattering and computational modeling. Biochemistry *37*, 8208–8217.
30. Kirchhofer, D., Eigenbrot, C., Lipari, M.T., Moran, P., Peek, P., and Kelley, R.F. (2001). The tissue factor region that interacts with factor Xa in the activation of factor VII. Biochemistry *40*, 675–682.
31. Dickinson, C.D., and Ruf, W. (1997). Active site modification of factor VIIa affects interactions of the protease domain with tissue factor. J. Biol. Chem. *272*, 19875–19879.
32. Bach, R., Gentry, R., and Nemerson, Y. (1986). Factor VII binding to tissue factor in reconstituted phospholipid vesicles: induction of cooperativity by phosphatidylserine. Biochemistry *25*, 4007–4020.
33. Leonard, B.J.N., Clarke, B.J., Sridhara, S., Kelley, R., Ofosu, F.A., and Blajchman, M.A. (2000). Activation and active site occupation alter conformation in the region of the first epidermal growth factor-like domain of human factor VII. J. Biol. Chem. *275*, 34894–34900.
34. Zur, M., and Nermerson, Y. (1978). The esterase activity of coagulation factor VII. J. Biol. Chem. *253*, 2203–2209.
35. Remington, S.J., Woodbury, R.G., Reynolds, R.A., Matthews, B.W., and Neurath, H. (1988). The structure of rat mast cell protease II at 1.9-Å resolution. Biochemistry *27*, 8097–8105.
36. Lamba, D., et al., and Bode, W. (1996). The 2.3 Å crystal structure of the catalytic domain of recombinant two-chain human tissue-type Plasminogen activator. J. Mol. Biol. *258*, 117–135.
37. Shobe, J., Dickinson, C.D., and Ruf, W. (1999). Regulation of the catalytic function of coagulation factor VIIa by a conformational linkage of surface residue Glu154 to the active site. Biochemistry *38*, 2745–2751.
38. Dickinson, C.D., Shobe, J., and Ruf, W. (1998). Influence of cofactor binding and active site occupancy on the conformation of the macromolecular substrate exosite of factor VIIa. J. Mol. Biol. *277*, 959–971.
39. Ruf, W. (1998). The interaction of activated factor VII with tissue factor: insight into the mechanism of cofactor-mediated activation of activated factor VII. Blood Coag. Fibrinolysis Suppl *9* S73–S78.
40. Bon, V.J., and Bertina, R.M. (1990). The contributions of Ca^{2+}, phospholipids and tissue-factor apoprotein to the activation of human blood coagulation factor X by activated factor VII. Biochem. J. *265*, 327–336.
41. Morrissey, J.H., Neuenschwander, P.F., Huang, Q.M., McCallum C.D., Su, B., and Johnson, A.E. (1997). Factor VIIa-tissue factor: functional importance of protein-membrane interactions. Thromb. Haemost. *78*, 112–116.
42. Kirchhofer, D., Lipari, M.T., Moran, P., Eigenbrot, C., and Kelley, R.F. (2000). The tissue factor region that interacts with substrates factor IX and factor X. Biochemistry *39*, 7380–7387.
43. Huntington, J.A., Read, R.J., and Carrell, R.W. (2000). Structure of a serpin-protease complex shows inhibition by deformation. Nature *407*, 923–926.
44. Mellet, P., and Bieth, J.G. (2000). Evidence that translocation of the proteinase precedes its acylation in the serpin inhibition pathway. J. Biol. Chem. *275*, 10788–10795.
45. Hopfner, K.-P., et al., and Bode, W. (1997). Converting blood coagulation factor IXa into factor Xa: dramatic increase in amidolytic activity identifies important active site determinants. EMBO J. *16*, 6626–6635.
46. Otwinowski, Z., and Minor, W. (1996). Processing of X-ray diffraction data collected in oscillation mode. Methods in Enzymol. *276*, 307–326.
47. CCP4 (Colaborative Computational Project 4) (1994). The CCP4 suite: programs for protein crystallography. Acta Crystallogr. D *50*, 760–763.
48. Navaza, J. (1994). AMoRe: an automated package for molecular replacement. Acta Crystallogr. A *50*, 157–163.
49. McRee, D.E. (1993). *Practical Protein Crystallography*. (San Diego, CA: Academic Press).
50. Laskowski, R.A., MacArthur, M.W., Moss, D.S., and Thornton, J.M. (1993). PROCHECK: a program to check the stereochemical quality of protein structures. J. Appl. Cryst. *26*, 283–291.

Accession Numbers

The X-ray crystallographic coordinates of A-183/rf7 have been deposited in the Protein Data Bank under accession code 1JBU.